



Effects of Zn and Sb Additions on Microstructure, Creep Behavior and Thermal Properties of Binary Eutectic Sn-0.7% Cu Lead-Free Solder

A.M. Yassin

Physics Department, Faculty of Education, Ain shams university, Cairo, Egypt

Received 16th July 2018
Accepted 31st March
2019

The effects of Zn and Sb additions on microstructure, creep behavior and thermal properties of binary eutectic Sn-0.7% Cu lead-free solder were investigated. Results show that Zn-addition reduced the melting temperature of Sn-0.7Cu and enhanced the creep resistance due to the formation of Cu_5Zn_8 intermetallic compound (IMC) and reduction of Cu_6Sn_5 phase in β -Sn matrix. Conversely, the Sb-addition showed a negative effect on both the creep resistance and melting temperature compared to the plain Sn-0.7 Cu and Sn-0.7 Cu-2.0 Zn alloys due to the formation of SnSb IMC particles and coarse Cu_6Sn_5 phase through the β -Sn rich phase. The average stress exponents of 4.9-6.0 and activation energies of 50-60 KJ/mol were obtained for three solders; suggesting that the dislocation climb controlled by lattice diffusion is the dominant creep mechanism. X-ray diffraction (XRD) analysis revealed that the lattice parameters (a), (c), the axial ratio (c/a) and the peak height intensities (hkl) of some crystallographic planes are changed with alloying additions and the crystallite size is decreased.

Keywords: Pb-free solders, Thermal properties, Microstructure, Alloying element additions, creep, X-ray analysis

Introduction

Recently, a lot of efforts have been made to replace the conventionally used SnPb solders by new Pb-free alloys due to the considerable toxicity of lead (Pb) on health and environment. The Sn-Cu based alloys are one of the families of promising Pb-free candidates due to their low cost and good mechanical properties and electrical conductivity. Nevertheless, the eutectic Sn-0.7Cu has a high melting temperature of 227°C, which is still a problem of Sn-Cu alloys [1]. Improving the physical properties of Pb-free alloys has been obtained by modification of chemical composition and addition of minor elements as well as the development of new processing routes by means of rapid solidification and mechanical alloying [2]. Huang et.al studied the creep properties of

three precipitation-strengthened Sn-based Pb-free solder alloys (Sn-0.7Cu, Sn-3.5Ag and Sn-3.8Ag0.7Cu) at constant applied stress of 17.5 MPa and working temperature of 348 K. They found that Sn-0.7Cu has the lowest creep resistance compared with the other two alloys [3]. The creep behavior of Sn-0.7Cu alloy with small amounts of inter-metallic compound (IMCs) of Cu_6Sn_5 particles in the β -Sn matrix has been studied by Wu and Huang [4]. They indicated that the creep rates are controlled by the dislocation pipe diffusion in Sn matrix. Microstructure studies at different cooling rates on different compositions of Sn-Cu alloys (Sn-0.5wt% Cu, Sn-0.7wt% Cu, Sn-0.9 wt.% Cu) showed that the Sn-Cu system is a weakly irregular eutectic system due to the formation of Cu_6Sn_5 IMCs with two different

eutectic morphologies (coarse and fine) during eutectic growth [5]. The indentation creep tests of Sn-Cu alloys (1 - 5wt. % Cu) has been investigated and concluded that the composition of Sn-4wt. % Cu solder alloy exhibited the greatest creep resistance [6]. The addition of In element enhanced the indentation creep of Sn-0.7 wt. % Cu solders [7]. The improvement of wettability, mechanical characteristics and creep resistance Sn-Cu alloys by introduction of a small amount of alloying elements were proposed by many researchers [8-9]. The addition of 0.5% rare earth elements (REE) to the Sn-0.7%Cu binary alloy improves the microstructures and refines both the β -Sn grains and the Cu_6Sn_5 IMCs in addition to their attractive mechanical properties (hardness, and creep resistance) [8]. Adding of Ag or In-element to Sn-0.7Cu solder decreased the melting temperature (T_m) from 227°C to 224°C and 217°C, respectively and increased the creep resistance compared to the plain alloy [10-12]. Alam et.al studied the effect of adding (2, 2.5 and 4.5) wt. % Ag to Sn-0.7Cu eutectic alloy on the microstructure, mechanical properties (hardness) and thermal properties. They found reduction in melting temperature from 234.88°C to 226.89 °C and increasing in the hardness, while by adding Ag up to 2.5 wt.% the hardness was decreased [13]. Also, the addition of Ni, Co, Ga, In, Bi or rare earth elements into Sn-0.7Cu solder showed improvement of hardness [14]. Ning Zhao et. al [15] indicated that after doping Ce element in Sn-0.7 Cu solder, the melting temperature was increased although the wettability was improved. The effect 0.08 wt.% Ni-addition on the microstructure and the mechanical properties of Sn-0.7 Cu alloy has been studied by Gyenes et. al [16]. They found that Sn-0.7 Cu-Ni alloy becomes fully eutectic [β -Sn + $(\text{Cu,Ni})_6\text{Sn}_5$], and the ultimate tensile strength (UTS), yield strength (YS) and hardness (HV) were increased. However, above a certain level of additions, their values were decreased whereas, the elongation was significantly increased with the appearance of large primary $(\text{Cu, Ni})_6\text{Sn}_5$ (IMCs). Taruk et. al [17] showed that the addition of 0.5wt.% Zn to the Sn-Cu eutectic alloy increases the hardness and YS, but slightly lowers the creep resistance. They also found that the addition of Bi decreases both the creep resistance and fracture time. In general, the effect of the primary phase (Cu_6Sn_5) on the creep behavior of Sn-rich is very essential in designing better solder alloy and in

understanding the deformation mechanism. However, there is seldom systematic data on the effect of Zn or/ and Sb additions on eutectic Sn-Cu solder alloys. In this research, 2.0 wt.% Zn and Sb were added into Sn-0.7Cu alloys. In order to obtain Sn-0.7Cu solder with good creep resistance, the microstructures and creep properties were studied and discussed in this paper to confirm the requirements of performance, melting temperature and pasty range were also discussed.

Experimental Work

Three solder alloys of compositions Sn-0.7wt.%Cu, Sn-0.7wt.%Cu-2wt.%Zn and Sn-0.7 wt.% Cu-2 wt.% Sb were prepared from high purity (99.99 wt%) component materials. The chemical compositions of three alloys are given in **Table (1)**.

Table (1): Chemical compositions of the studied solders (wt.%)

Alloy	Cu	Sb	Zn	Sn
Sn-0.7Cu	0.7	-	-	Bal.
Sn-0.7Cu-2Sb	0.7	2.0	-	Bal.
Sn-0.7Cu-2Zn	0.7	-	2.0	Bal.

To ensure the dissolution of Sn, Cu and Sb or Zn; the materials were melted at 600 °C for 30 min and then poured in a steel mold to produce the chill cast ingot. The solder ingots were mechanically machined into wire samples with a gauge length of 5×10^{-2} m and 1.2×10^{-2} m in diameter. The samples were annealed at 150°C for 120 min, then left to cool slowly to room temperature with cooling rate of 10°C /s to obtain samples containing fine microstructure, fully precipitated phases and free from any plastic strain accumulation during machining. Creep testing was done at three working temperatures (298, 343 and 393K) monitored by a thermocouple contacting with the specimen (within accuracy of $\pm 1^\circ\text{C}$) and under constant applied stresses using a computerized testing machine. To understand the melting process of three solder alloys; differential scanning Calorimetry (Shimadzu DSC-50) (DSC) was carried out at heating rate of (10°C/min.) in Ar flow. The microstructure was investigated by X-ray diffraction (XRD) using Philips X' Pert (MPD) Goniometer PW3050/00 with graphite monochromatic using Cu-K_α target and Ni filter operated at (40 K.V.) and (30 mA) to give radiation of a wave length ($\lambda = 0.15406$ nm) has been carried out to identify the phases of alloy

samples with diffraction angles (2θ) from 25° to 90° . Morphological studies have been conducted using both optical microscopy (OM) and scanning electron microscopy (SEM) after using an etching solution of 2% HCl, 3% HNO₃ and 95% (vol. %) ethyl alcohol.

Results and Discussion

X-ray diffraction analysis

X-ray diffraction investigations of Sn-0.7 Cu, Sn-0.7 Cu-2.0 Zn and Sn-0.7 Cu-2.0 Sb LFSAs were studied to identify the phases formed through the solder matrix. **Figure (1a)** shows the XRD results of three alloys, which show: (i) large peaks intensity of β -Sn-rich phase, (ii) small peaks of Cu₆Sn₅ phases through the entire solders.

The microstructure of Zn- and Sb-containing solders shows additional IMCs of Cu₅Zn₈ and SnSb, respectively, dispersed in β -Sn rich matrix **Fig. (1 b and c)**. From the XRD analysis of Zn-containing solder, the intensity of β -Sn peak at 43.565° was increased while the peak of the Cu₆Sn₅ at 42.725° was decreased compared to the plain solder due to the formation of Cu₅Zn₈ IMCs in agreement with the previous work [18, 19]. **Figure (1 c)** shows the formation of SnSb IMC through the β -Sn matrix in addition to the small peak of Cu₆Sn₅ IMCs. Moreover, the intensities of β -Sn and Cu₆Sn₅ phases were found to decrease with the addition of either Zn or Sb elements. X-

ray lattice parameters (a & c) for the three alloys have been calculated and listed in **Table (2)**.

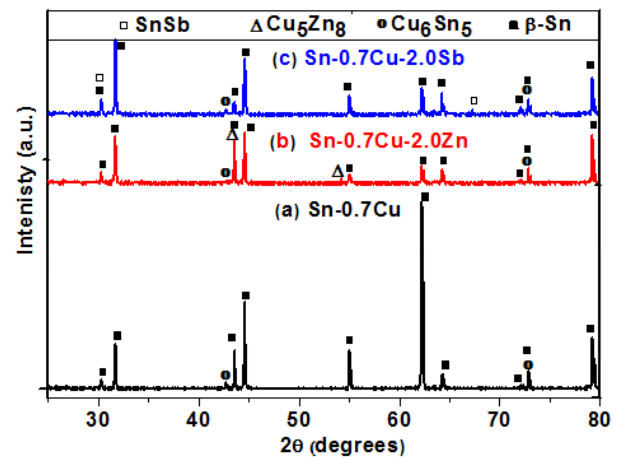


Fig. (1): X-Ray Diffraction of (a) Sn-0.7Cu, (b) Sn-0.7Cu-2.0Zn and (c) Sn-0.7Cu-2.0Sb lead free solder alloys

The results show that all parameters are sensitive to Zn or Sb additions. The apparent crystallite size (L) for the main reflections (101) & (112) planes after resolution of $K_{\alpha 1}$ & $K_{\alpha 2}$ intensities was calculated from the half maximum full width (HMF_W) as shown in **Fig. 2**. For (112) reflection (as an example) and by using Sherrer equation (1) [20, 21], the crystallite sizes are tabulated in **Tables (3 a and b)**.

$$L = K\lambda / B \cos \theta \quad (1)$$

Where, K is Sherrer parameter equal to (0.9) for (HMF_W)

Table (2): X-ray parameters

Parameter	Sn-0.7Cu	Sn-0.7Cu-2Zn	Sn-0.7Cu-2Sb
a	5.8373 ± 0.0011	5.8158 ± 0.0014	5.8389 ± 0.0012
c	3.3151 ± 0.0081	3.1867 ± 0.0094	3.1836 ± 0.0008
c/a	0.567918	0.54794	0.545232

Table (3 a): The crystallite size of (112) reflection

Sample	Crystallite size [L(nm)] of (112) reflection of Sn-0.7Cu, Sn-0.7Cu-2.0Zn and Sn-0.7Cu-2.0Sb solders
Sn-0.7Cu	145.0
Sn-0.7Cu-2Zn	101.7
Sn-0.7Cu-2Sb	134.0

Table (3 b): The crystallite size of (101) reflection

Sample	Crystallite size [L(nm)] of (101) reflection of Sn-0.7Cu, Sn-0.7Cu-2.0Zn and Sn-0.7Cu-2.0Sb alloys
Sn-0.7Cu	102.5
Sn-0.7Cu-2Zn	84.6.0
Sn-0.7Cu-2Sb	101.4

The results show that L was decreased with the additions of either Zn or Sb elements. The Zn-containing solder has the smallest crystallite size (84.6 and 101.7nm) compared to 102.5 and 145nm of the plain solder alloy for both (101) and (112) planes, respectively. Alloying with Sb element shows a less decrease in crystallite sizes. These results explained the higher creep resistance of the Zn-containing compared to that of Sb-containing solder.

Thermal analysis

A high-quality solder alloys should have a lower melting temperature and a narrow pasty range for electronic applications [22]. Thus, the melting temperature as a physical property is very important. **Figure (3 a-c)** shows the DSC curves of Sn-0.7Cu, Sn-0.7Cu-2.0Zn and Sn-0.7Cu-2.0Sb solders.

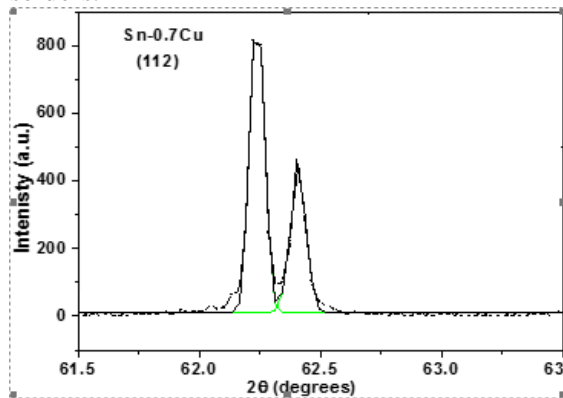


Fig. (2): Resolution of (112) plane

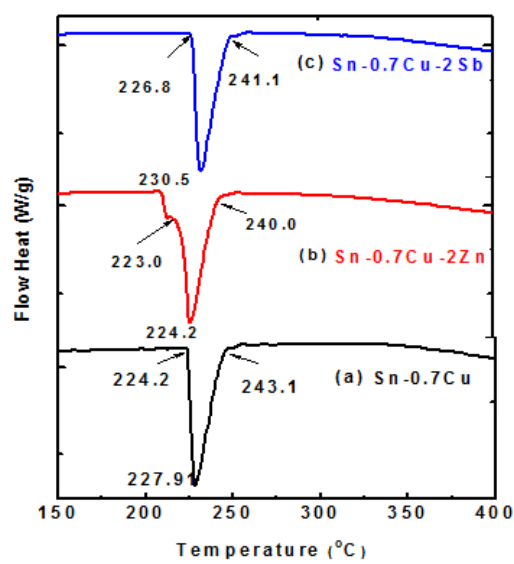


Fig. (3): DSC curves of (a) Sn-0.7Cu (b) Sn-0.7Cu-2.0Zn (c) Sn-0.7Cu-2.0Sb solder

In **Fig. (3 a)**, the eutectic temperature of Sn-0.7Cu solder at the endothermic peak is 227.9°C, which is in quite agreement with the previous work [10]. With the addition of 2Zn to Sn-0.7Cu alloy, the endothermic peak temperature was significantly reduced to 224.2 °C owing to the dissolution of small amount of Cu_6Sn_5 in the β -tin matrix, as seen in **Fig. (3 b)**. The eutectic temperature of Sn-0.7Cu solder alloy containing 2wt%Sb was increased from 227.9°C to 230.5 °C as shown in **Fig. (3 c)**. The increase in endothermic peak was attributed to the formation of SnSb cuboids (confirmed by EDS analysis) as IMC particles, which float at the surface of solder during solidification before the formation of Cu_6Sn_5 in β -tin matrix [23]. The pasty range, which is the difference between solidus (T_{onset}) and liquidus temperatures (T_{end}), was found to decrease with Zn or Sb addition from 18.9°C to 17 °C and 14.2 °C, respectively. The heat of fusion (ΔH) equation for any material [24] is given by:-

$$\Delta H = \frac{KA}{m} \quad (2)$$

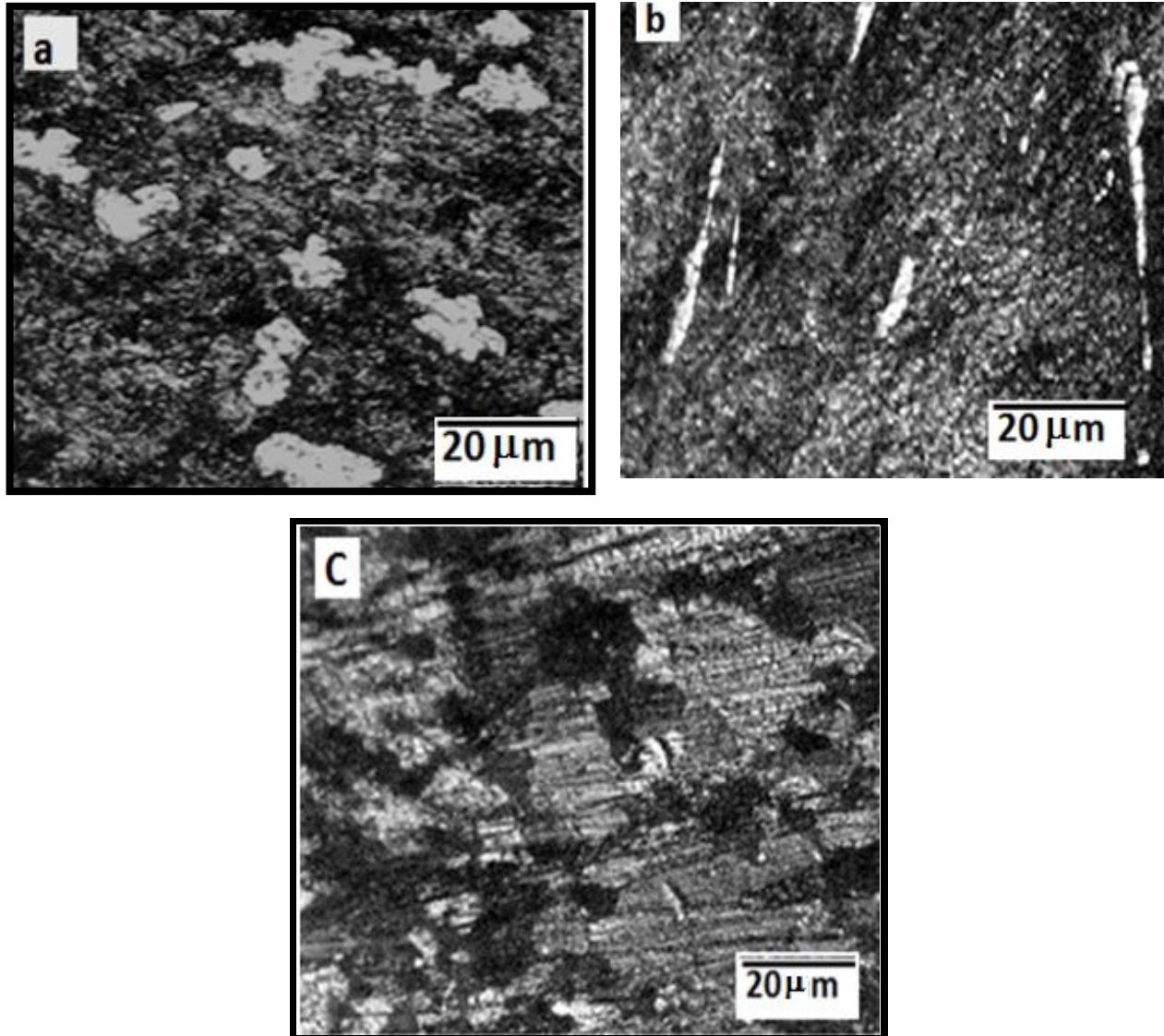
Where, K is constant depends on a crucible shape of the DSC system, m is the sample mass and A is the area under the endothermic peak. **Table (4)** listed the values of T_{onset} , T_{end} , pastry ranging ($T_{\text{end}} - T_{\text{onset}}$), and ΔH of three solders. The results showed that the addition of Zn to the eutectic Sn-0.7 Cu solder reduced the eutectic temperature from 227.91 °C to 224.20 °C and decreased both of the pastry ranging from 18.9 – 17.0 and the heat of fusion from 45.48 to 35.36 J/g, which indicated that the Zn-containing solder is the best solder for saving energy.

The effect of Zn and Sb additions on microstructure

Microstructure plays a vital role to create high quality solder alloys and to explain their mechanical behavior. **Figure (4 a)** shows an OM microstructure of Sn-0.7 Cu solder with a gray phase of Cu_6Sn_5 particles and dark phase of β -Sn matrix besides the eutectic phase. The addition of 2 wt.% Zn into Sn-0.7Cu solder refined the Cu_6Sn_5 particles and created a fine IMCs of Cu-Zn phase through β -Sn matrix as shown in Fig. (4 b), which is confirmed by EDS investigation shown in **Fig. (5 e)**. Conversely, the addition of 2 wt.% Sb created new IMC particles of SnSb (gray phase), besides the formation of Cu_6Sn_5 IMC (bright) through the β -Sn matrix (**Fig. 4 c**).

Table (4): The DSC results of Sn-0.7Cu, Sn-0.7Cu-2Zn and Sn-0.7Cu-2Sb solders

Alloy	T _{onset} (°C)	T _{end} (°C)	Melting temperature (°C)	Pastry range (°C)	ΔH (J/g)
Sn-0.7Cu	224.20	243.10	227.91	18.90	45.48
Sn-0.7Cu-2Zn	223.00	240.00	224.20	17.00	35.36
Sn-0.7Cu-2Sb	226.80	241.10	230.50	14.20	39.43

**Fig. (4): OM micrographs of (a) Sn-0.7 Cu, (b) Sn-0.7 Cu-2.0Zn and (c) Sn-0.7 Cu-2.0 Sb solder alloys**

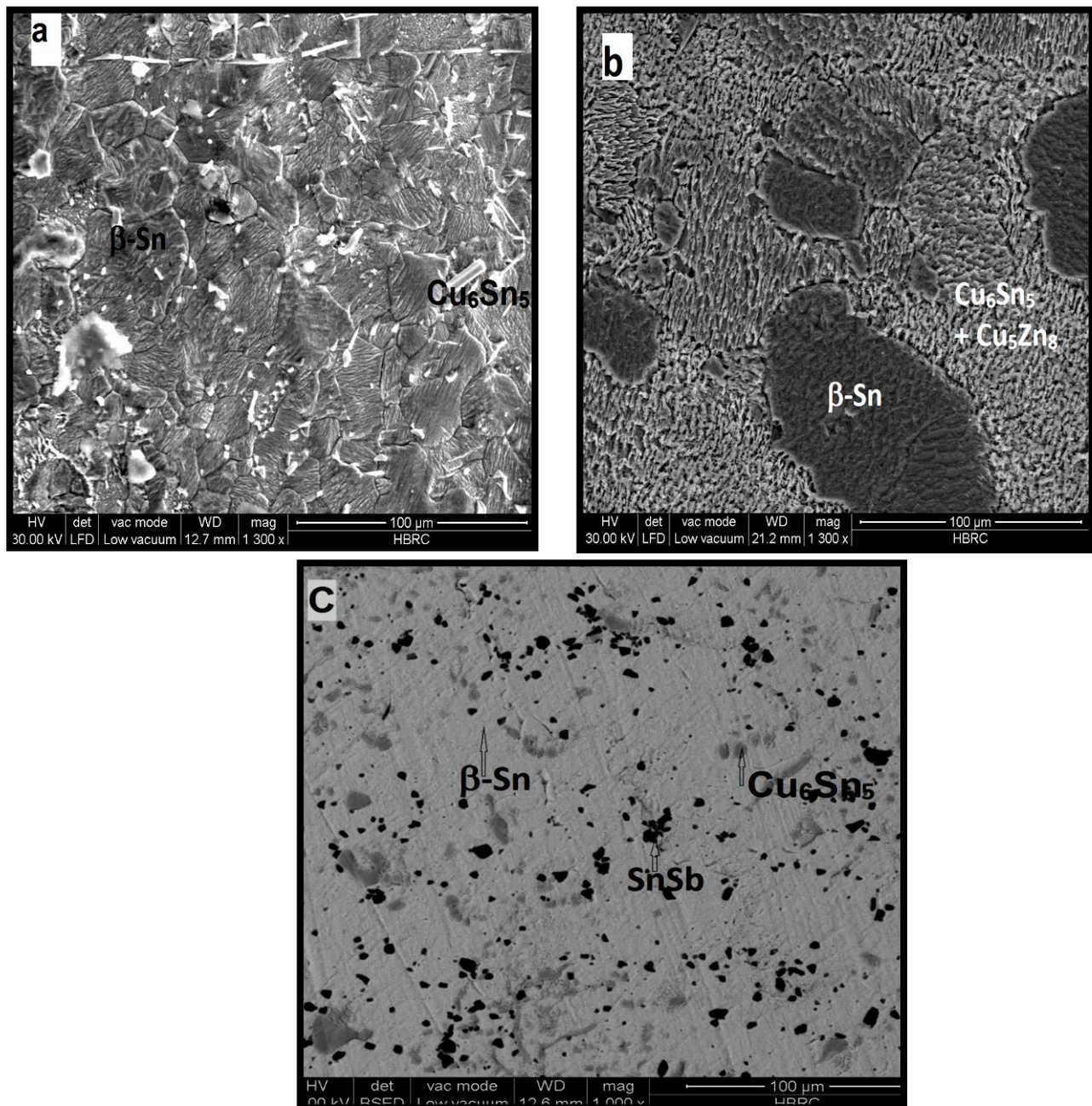


Fig. (5): Shows SEM micrographs of (a) Sn-0.7 Cu (b) Sn-0.7 Cu-2.0 Zn and (c) Sn-0.7 Cu-2.0 Sb solders

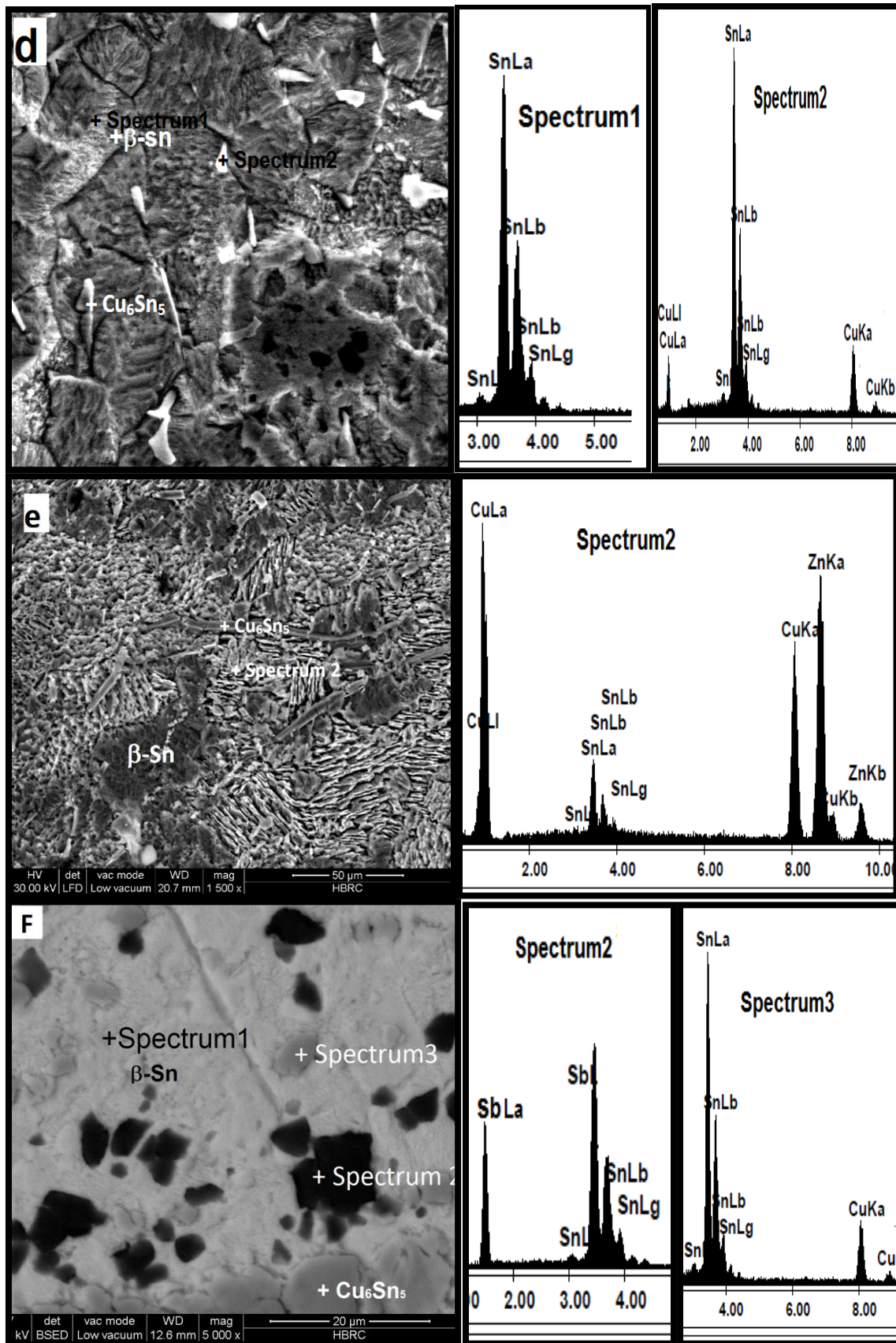


Fig. (5 d, e, f): Shows SEM, EDX micrographs of (d) Sn-0.7Cu (e) Sn-0.7 Cu-2.0 Zn and (f) Sn-0.7 Cu-2.0 Sb solders

Figure (5 a, b, c) shows SEM micrographs as a comparison of microstructures between Sn-0.7Cu, Sn-0.7Cu-2.0Zn and Sn-0.7Cu-2.0Sb alloys. **Figure (5 d)** shows the high magnification microstructure of Sn-0.7Cu solder, which consists of two phases: (i) needle-like Cu_6Sn_5 particles of $0.9\mu\text{m}$, (ii) the β -tin grains ($15\mu\text{m}$) as identified by EDS analysis and x-ray diffraction (**Fig. 1 a**). The EDS results in **Fig. (5 e)** shows that the addition of 2.0% Zn to Sn-0.7Cu alloy leads to the formation of new fiber-like Cu_5Zn_8 IMCs ($0.5\mu\text{m}$) and reduced the needle-like Cu_6Sn_5 ($0.3\mu\text{m}$) phase in β -tin matrix. The results are in agreement with previous works [18, 19, 25]. The presence of the small particle size of Cu_6Sn_5 and Cu_5Zn_8 in β -tin matrix are confirmed by the EDS (**Fig. 5 e**) and X-ray diffraction patterns (**Fig. 1 b**). The IMCs Cu_6Sn_5 and Cu_5Zn_8 could act as obstacles, which resist the motion of dislocations. The addition of 2.0% of Sb to Sn-0.7 Cu creates a new phase of SnSb cuboids ($2.0\mu\text{m}$) of IMCs besides the Cu_6Sn_5 ($1.2\mu\text{m}$) particles extended in the β -tin matrix as confirmed by EDS (**Fig. 5 f**) and X-ray diffraction (**Fig. 1 c**). The SEM investigations also showed a less amount of Cu_6Sn_5 IMCs in Sn-0.7Cu-2.0Sb than that of Sn-0.7Cu and Sn-0.7Cu-2.0Zn solders due to the formation of SnSb phase at the beginning of solidification process before the Cu_6Sn_5 particles formation. **Figure (5 f)** shows gray particles of Cu_6Sn_5 and dark particles of SnSb through β -tin phase. The particle sizes of all phases have been calculated and listed in **Table (5)**. The results show that the addition of Zn and Sb increased the β -Sn grain size ($18 - 35\mu\text{m}$); whereas the addition of Zn created a new small size of Cu_5Zn_8 particles ($0.5 \mu\text{m}$) and reduced the Cu_6Sn_5 particle size from $0.9 \mu\text{m}$ to $0.3\mu\text{m}$. The Sb-addition created SnSb IMCs with an average size of $\sim 2.0\mu\text{m}$ and increased the Cu_6Sn_5 particles size to $\sim 0.9 - 1.2 \mu\text{m}$. The growth in particles size of Sn-0.7 Cu-Sb leads to initiate small cracks during creep tests, which explains the decrease in its creep resistance and fracture time.

Creep properties

Creep curves for the three solder alloys were carried out at three working temperatures (298K, 343K and 393K) and under different applied stresses (7.8–19.6 MPa). **Figure (6 a-c)** shows the creep behavior of Sn-0.7Cu, Sn-0.7Cu-2.0Zn

and Sn-0.7Cu-2.0Sb solder materials tested at 298, 343 and 393K and under constant applied stress (12.7, 11.7 and 9.8 MPa), respectively. On the other hands, **Fig. (6 d)** presents the effect of different applied stresses at 298K on Sn-0.7Cu alloy.

Figure (7 a-c) shows the creep rate-time curves at different temperatures and loads for Sn-0.7 Cu, Sn-0.7 Cu-2.0 Zn and Sn-0.7 Cu-2.0Sb, respectively. Typical creep curves consist of three stages; primary (transient) creep, secondary (steady state) creep and tertiary creep (fracture stage). They indicated that the Sn-0.7 Cu-2.0 Zn has the lowest creep rate followed by Sn-0.7 Cu, whereas the highest creep rate was for Sn-0.7 Cu-2.0Sb alloy. The effect of Zn-addition to the microstructure of Sn-0.7 Cu solder alloy creates a new IMCs of Cu_5Zn_8 with $0.5 \mu\text{m}$ size besides reducing the needle size of Cu_6Sn_5 ($0.3 \mu\text{m}$) inside the β -Sn matrix. The presence of fine dispersive Cu_5Zn_8 & Cu_6Sn_5 particles could act as a pinning effect to the dislocation motion, which enhanced the creep resistance of Zn-containing solders. The microstructure of Sb-containing solders consists of cuboids of SnSb ($2.0 \mu\text{m}$) and large size of Cu_6Sn_5 ($1.2 \mu\text{m}$) in the β -Sn matrix. During the creep process, the coarse (SnSb and Cu_6Sn_5) IMCs creates a crack propagation path [26], which leads to a decrease in the creep resistance of Sn-0.7Cu-2.0Sb solder.

Transient creep

Using the transient creep equation [27]

$$\varepsilon_{tr} = \beta t^n \quad (3)$$

$$\ln \varepsilon_{tr} = \ln \beta + n \ln t \quad (4)$$

Where, n and β are the transient creep parameters that depend on both the working temperature and applied stress. The parameter n usually has a value in the range of $0 < n < 1$. **Figure (8 a- c)** shows the relations between $\ln \varepsilon_{tr}$ against $\ln t$ for wire specimens of the Sn-0.7 Cu, Sn-0.7 Cu-2Zn and Sn-0.7 Cu-2Sb tested at (298K, 12.7 MPa), (343 K, 11.7 MPa) and (393 K, 9.8 MPa), respectively.

Table (5): Phases particle size of Sn0.7Cu, Sn0.7Cu-2zn and Sn0.7Cu-2Sb alloys

Alloy	β -tin	Particle Size (μm)		
		Cu_6Sn_5	Cu_5Zn_8	SnSb
Sn-0.7Cu	18	0.9	-	-
Sn-0.7Cu-2.0Zn	25	0.3	0.5	-
Sn-0.7Cu-2.0Sb	35	1.2	-	2.0

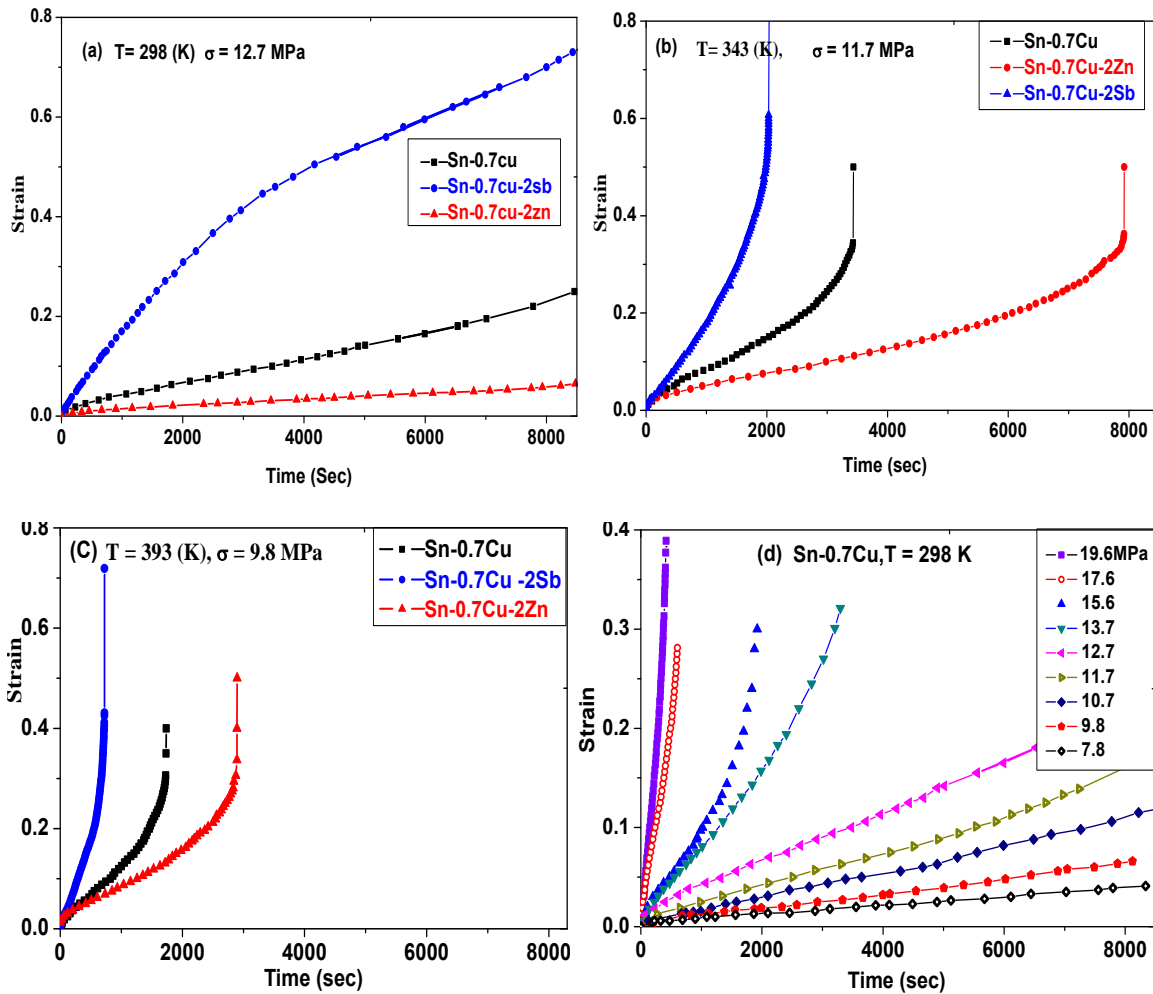


Fig. (6): Shows the creep behavior at (a) 298K, 12.7 MPa, (b) 343K, 11.7 MPa, (c) 393K, 9.8 MPa for Sn-0.7 Cu, Sn-0.7 Cu-2.0 Zn and Sn-0.7 Cu-2.0Sb and (d) 298K for Sn-0.7 Cu solder under different applied stresses

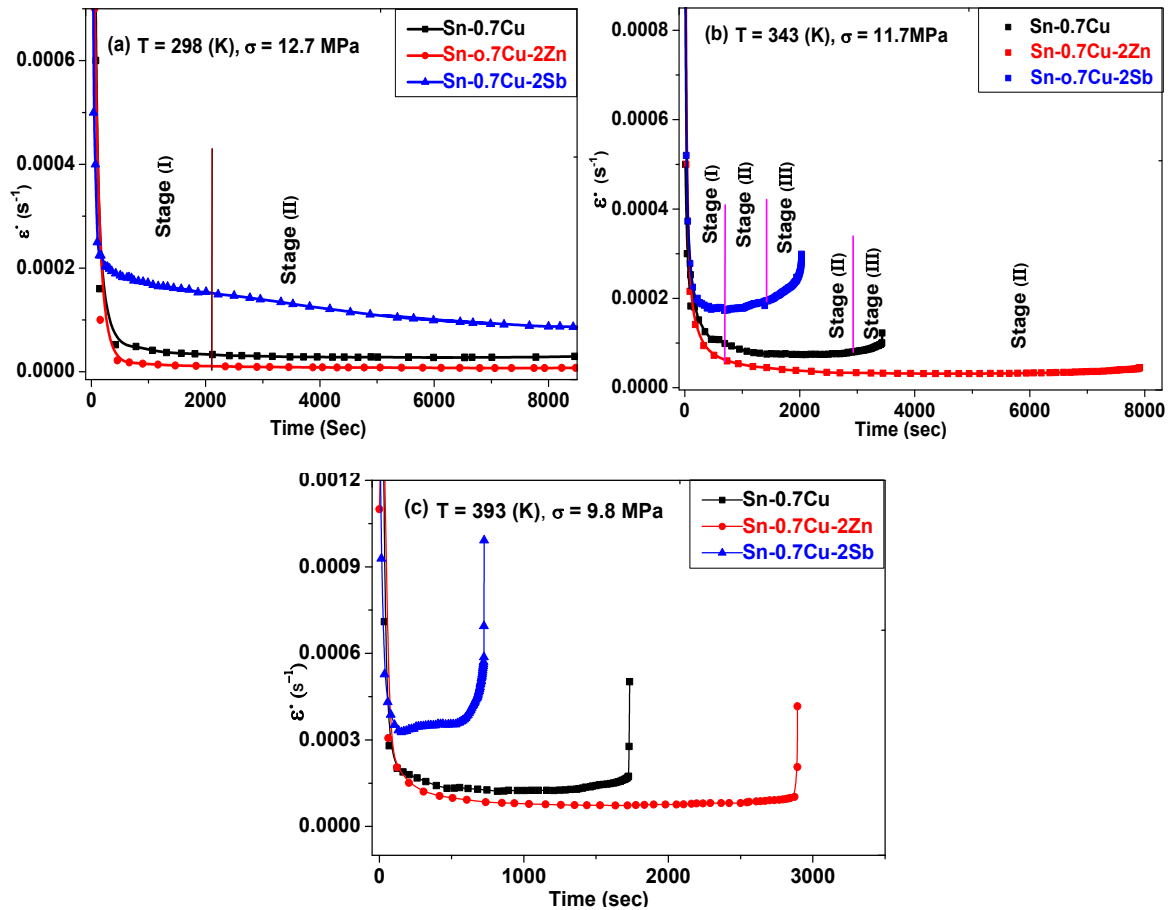


Fig. (7): shows strain rate - time relationships at a) 298 K, 12.7 MPa, (b) 343K, 11.7 MPa and (c) 393 K, 9.8 MPa for Sn-0.7 Cu, Sn-0.7Cu-2.0 Zn and Sn-0.7 Cu-2.0Sb solders

The transient creep mechanism in stage I depends on β and n parameters obtained from the relation between $\ln \dot{\epsilon}_{tr}$ and $\ln t$ (Fig. 7 a - c). The calculated parameters are listed in Table (6).

Figure (9 a, b) shows that the transient parameters n and β depend on both of creep test temperature and solder addition, which attributed to the change in the microstructure. It is clear that the increase in the parameter n and the decrease in β at the high temperature (393 K) may be attributed to the generation of new dislocations through the dislocation network.

Steady state parameters

of steady state creep rate $\dot{\epsilon}_s$ on the applied stress (σ) and temperature T can be expressed using Norton power law [28]:

$$\dot{\epsilon}_s = A \sigma^m \exp(-Q/RT) \quad (5)$$

$$\ln \dot{\epsilon}_s = \ln A + m \ln \sigma - Q/RT \quad (6)$$

Where, A is constant depends on the material structural properties, m is the stress exponent. At a given temperature, the creep stress exponent (m) can be calculated from the relation between $\ln \sigma$ against $\ln \dot{\epsilon}_s$, and the activation energy (Q) can be obtained from the relation between $\ln \dot{\epsilon}_s$ against $\ln(1000/T)$. Figure (10) shows the dependence of stress exponent (m) on the creep test temperatures and alloying element additions.

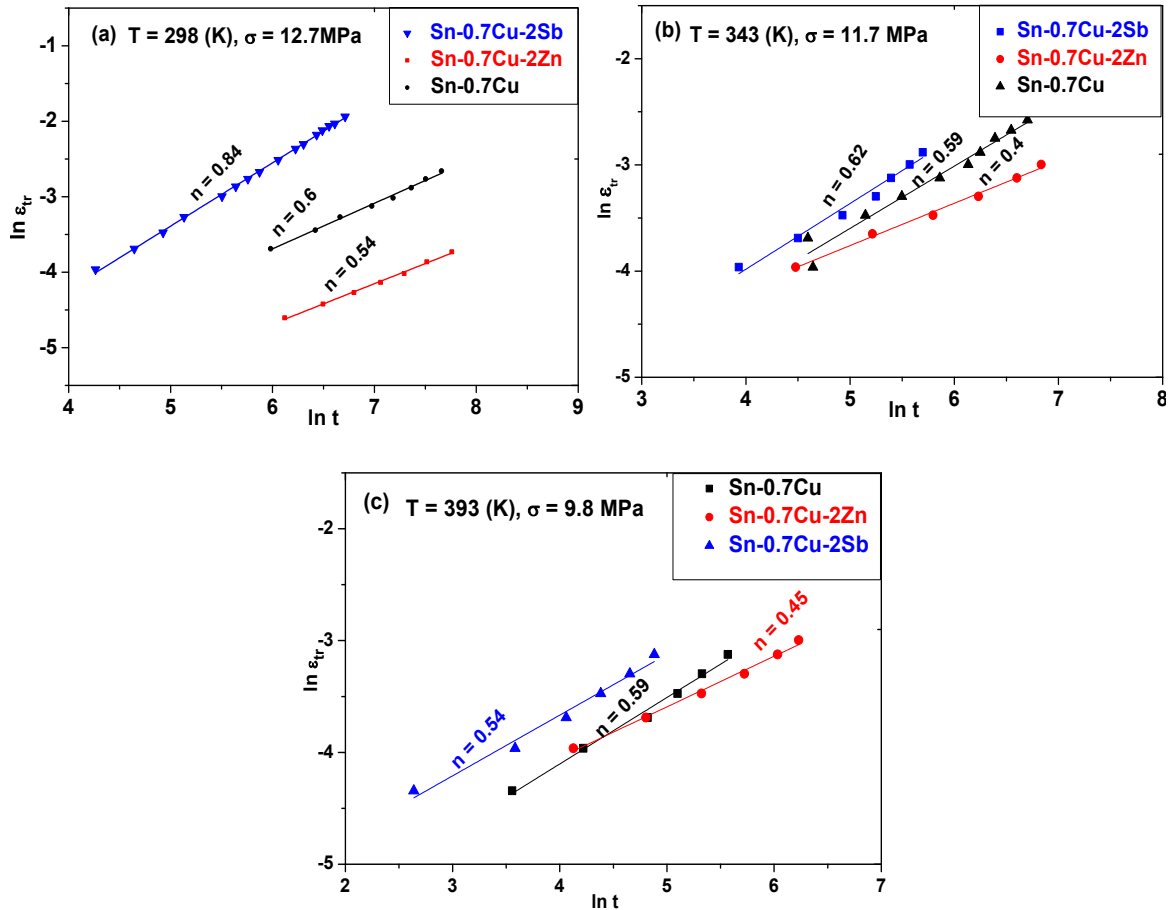


Fig. (8): Shows the relations between $\ln \varepsilon_{tr}$ against $\ln t$ for Sn-0.7 Cu, Sn-0.7 Cu-2Zn and Sn-0.7 Cu-2Sb alloys tested at (a) 298K, (b) 343K and (c) 393K

Table (6): Transient parameters (n & β)

Solder alloy	298 (K)		343 (K)		393 (K)	
	n	β	n	β	n	β
Sn-0.7Cu	0.60	-7.30	0.59	-6.50	0.59	-6.50
Sn-0.7Cu-2.0Zn	0.54	-7.90	0.40	-5.80	0.45	-5.90
Sn-0.7Cu-2.0Sb	0.84	-7.58	0.62	-6.50	0.54	-5.80

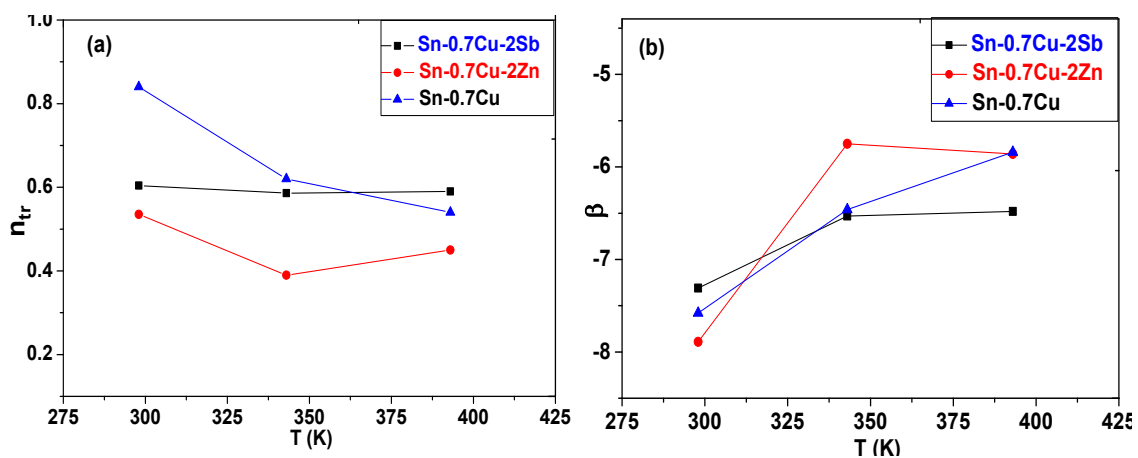


Fig. (9): Dependence of (a) the exponent (n_{tr}) and (b) the exponent (β) on the working temperature for Sn-0.7 Cu, Sn-0.7 Cu-2 Zn and Sn-0.7 Cu-2Sb alloys

Table (7) indicates that by increasing the working temperature; the stress exponent (m) decreases and, in the same time, becomes very sensitive with the solder additions. The estimated m values of the Sn-0.7Cu solder at 298, 343 and 393K were 5.8, 5.2 and 4.3, which are in agreement with the obtained values by El-Daly et.al [14].

Table (7): Stress exponent values (m) and activation energy (Q) for Sn-0.7 Cu, Sn-0.7 Cu-2.0 Zn and Sn-0.7 Cu-2.0 Sb alloys

The stress exponent m plays an important role to identify the mechanisms controlling the deformation process; ($m \approx 3$ represents a viscous glide and $m \geq 4$ dislocation climb [29]). The experimental results show that the Sn-0.7Cu, Sn-0.7Cu-2Zn and Sn-0.7Cu-2Sb solders have the stress exponents m ; (5.8, 5.2, 4.3), (7.0, 5.9, 5.1) and (5.3, 5.0, 4.5) correspond to the test temperatures 298K, 343K and 393K, respectively. The values of m suggest that the creep deformation mechanism is the dislocation climb, which attributed to the precipitation - strengthening of the

Cu_6Sn_5 , Cu_5Zn_8 and SnSb IMCs as shown in **Table (7)**. **Figure (11)** shows the linear relationship of strain rate–temperature dependence. The calculated values of m and Q are listed in **Table (7)**.

It is clearly shown that the m value decreases at constant temperature with the addition of Sb-element to Sn-0.7 Cu alloy, which was attributed to the change of microstructure due to the formation of SnSb particles and the coarsening of the Cu_6Sn_5 (IMCs) through β -Sn matrix. The Zn-containing solder shows an increasing in the stress exponent (m) values (4.3-7.0); due to the refining of Cu_6Sn_5 IMCs. Also, the m values decrease by increasing the working temperature owing to the instability of microstructure. The Q value of plain solder is ~ 55 KJ/mol, which increased to ~ 60 KJ/mol with Zn addition, but decreased to ~ 50 KJ/mol with the addition of Sb-element. On the basis of the stress exponent and the activation energy values; it is suggested that dislocation climb creep is the dominant deformation mechanism controlled by lattice diffusion [30].

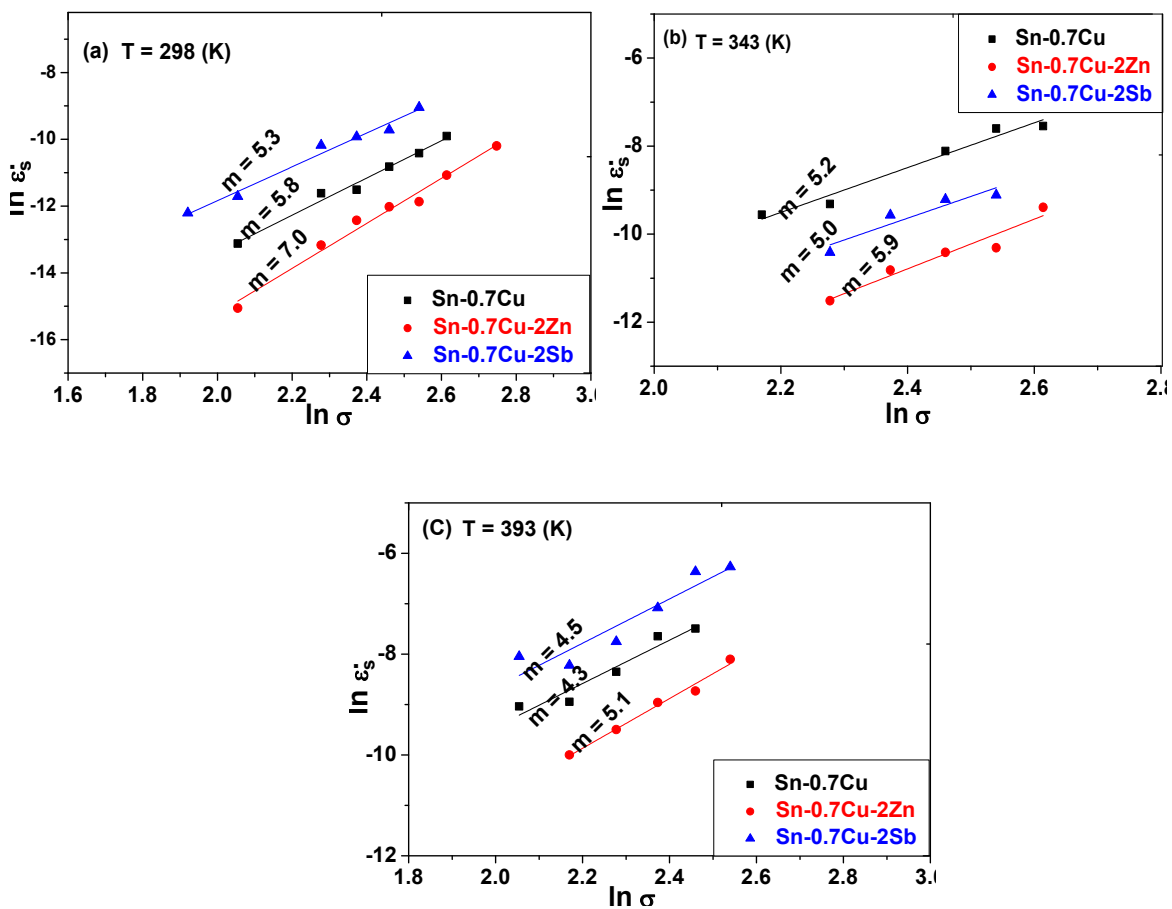


Fig. (10): The relation between $\ln \dot{\epsilon}_s$ against $\ln \sigma$ for Sn-0.7 Cu, Sn-0.7 Cu-2Zn and Sn-0.7 Cu-2Sb alloys at (a) 298 K, (b) 343 K and (c) 393 K

Table (7): Stress exponent values (m) and activation energy (Q) for Sn-0.7 Cu, Sn-0.7 Cu-2.0 Zn and Sn-0.7 Cu-2.0 Sb alloys

Alloy	Q (kJ/mol)	Temperature (K)	m
Sn-0.7Cu	55.0	298	5.8
		343	5.2
		393	4.3
Sn-0.7Cu-2.0Zn	60.0	298	7.0
		343	5.9
		393	5.1
Sn-0.7Cu-2.0Sb	50.0	298	5.3
		343	5.0
		393	4.5

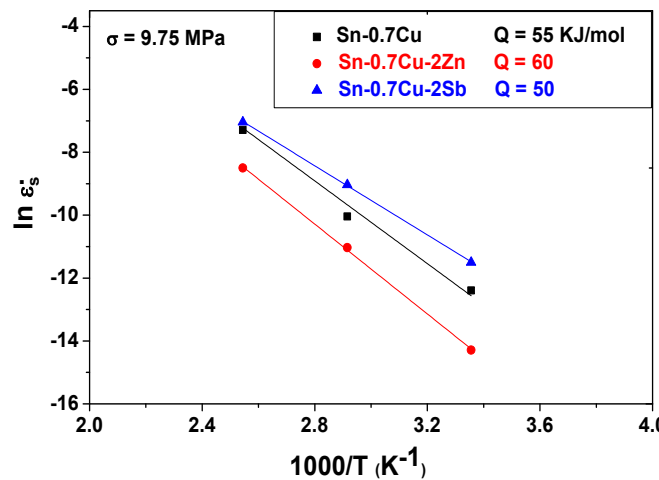


Fig. (11): Linear relationships of the strain rate-temperature of Sn-0.7 Cu, Sn-0.7 Cu-2Zn and Sn-0.7 Cu-2Sb alloys crept at 9.8 MPa

Conclusions

Three lead free solders Sn-0.7 wt.% Cu, Sn-0.7 wt.% Cu-2.0 wt. %Zn and Sn-0.7 wt.% Cu-2.0 wt.% Sb were conducted to analyze the effect of Zn and Sb additions on the microstructure, melting point and creep behavior of Sn-0.7 wt.% Cu solders. The conclusions are summarized as follows:

1. The Zn-containing solder showed a superior creep resistance due to the strengthening effect of fine dispersion Cu_6Sn_5 particles as well as the formation of the fine particles of Cu_5Zn_8 (IMCs) in β -Sn matrix.
2. The addition of Sb-element to Sn-0.7 Cu alloy increases the strain rate of the creep behavior, which attributed to the crack path creation as a result of the SnSb (IMCs) formation, the coarsening of Cu_6Sn_5 particles and the growth of β -Sn grain size.
3. Using the DSC investigations, the addition of Zn to Sn-0.7 Cu alloy decreased the melting point from 227.9 to 224.2°C although the addition of Sb element increased the melting point from 227.9°C to 230.9°C.
4. Unlike Sb-element addition, the transient exponents n of the plain alloy was decreased by increasing the testing temperature and the addition of Zn-element
5. The stress exponents (m) for lead-free solders are decreased by increasing the testing temperature due to the dissolution of the Cu_6Sn_5 phase at a high temperature.
6. On the basis of the average stress exponents 5.1, 6.0 and 4.9 and activation energies of 55.0 KJ/mol, 60.0 KJ/mol and 50.0 KJ/mol for Sn-0.7 Cu, Sn-0.7 Cu-2.0Zn and Sn-0.7Cu-2.0Sb solders respectively; the deformation mechanism is dislocation climb controlled by the lattice diffusion for all solders.

References

1. G. Zeng, S. Xue, L. Gao, L. Zhang, Y. Hu and Z. Lai, "Interfacial microstructure and properties of Sn-0.7Cu-0.05Ni/Cu solder joint with rare earth Nd addition", *J. Alloy Compd.*, 509, (2011), 7152-61.
2. Yu Chi - Yang, Wei - Yu Chen and Jeng-Gong Duh, "Suppressing the growth of Cu-Sn intermetallic compounds in Ni/Sn-Ag-Cu/Cu-Zn solder joints during thermal aging", *Intermetallics*, 26, (2012), 11-17.
3. M.L. Huang, C.M.L. WU and L. Wang, "Creep Resistance of Tin-Based Lead - Free Solder Alloys", *Journal of Electronic Materials*, 34, 11, (2005), 1373-1377.
4. C.M.L. Wu and M.L. Huang, "Creep Behavior of Eutectic Sn-Cu Lead- Free Solder Alloy", *J. Electronic Materials*, 31, 5, (2002), 442 - 448.
5. T. Ventura, S. Terzi, M. Rappaz and A.K. Dahle "Effects of solidification kinetics on microstructure formation in binary Sn - Cu solder alloys", *Acta Mater.*, 59 (4), (2011), 1651-1658.
6. A.F. Abd El-Rehim and H.Y. Zahran, "Microstructure evolution and mechanical properties of Sn0.7Cu0.7Bi lead-free solders produced by directional solidification", *Journal of Alloys and Compounds*, 295, (2017), 3666-3673.
7. M. Kamal and T. El-Ashram, "Micro-creep of rapidly solidified Sn-0.7wt%Cu-In solder alloys", *Mater. Sci. Eng., A*, 456, (2007), 1- 4.
8. C.M.L. Wu, D.Q. YU, C.M.T. Law, and L. Wang, "Microstructure and Mechanical Properties of New Lead-Free Sn-Cu-RE Solder Alloys", *Journal of Electronic Materials*, 31, 9, (2002), 928-932.
9. G. Li, Y. Shi, H. Hao, Z. Xia, Y. Lei and F. Guo, "Effect of phosphorus element on the comprehensive properties of Sn-Cu lead-free solder", *Journal of Alloys and Compounds*, 491, (2010), 382-385.
10. A.A. El-Daly and A.E. Hammad, "Enhancement of Creep Resistance and Thermal Behavior of Eutectic Sn-Cu Lead Free Solder Alloy by Ag and In-Additions", *Materials and Design* 40, (2012), 292-298.
11. A.A. El-Daly and A.E. Hammad, "Development of high strength Sn-0.7Cu Solders with the addition of small amount of Ag and In", *J. of Alloys and Compounds*, 509, (2011), 8554-8560.
12. S.I. Mudryi, I.I. Shtablayvi, V.I. Sklyarchuk, Y.O. Plevachuk, A.V. Korolyshyn and A.S. Yakymovych, "Structure and electric resistance of Sn-Cu(Ag) solders in the pre-crystallization temperature range", *Materials Science*, 46, 4, (2011), 464-472.
13. S.N. Alam, Prerna Mishra and Rajnish Kumar "Effect of Ag on Sn-Cu and Sn-Zn lead free solders" *Materials Science-Poland*, 33(2), (2015), 317-330.
14. Guang Zeng, Songbai Xue and Liang Zhang, "Recent Advances on Sn-Cu Solders with alloying elements", *J Matter Sci*, 22, (2011), 565-578.
15. Ning Zhao, M.L. Huang, Y. Zhong and H.T. Ma, "Effects of rare earth Ce addition on the microstructure, wettability and interfacial reactions of eutectic Sn-0.7Cu", *J. Mater. Sci.*, 26(1), (2014), 345-352.
16. Gyenes, A. Simon, P. Lanszki, Z. Gacsi, "Effects of Nickel on the microstructure and the mechanical properties of Sn-0.7Cu lead-free solders", *Archives of Metallurgy and Materials*, 60, 2, (2015), 1449-1454.
17. Tarek -Ashram and R.M. Shalaby, "Effect of Rapid Solidification and Small Additions of Zn and Bi on the Structure and Properties of Sn-Cu Eutectic Alloy", *Journal of Electronic Materials*, 34, 2, (2005), 212-215.
18. H.Y. Song, Q.S. Zhu, Z.G. Wang, J.K. Shang and M. Lu, "Effects of Zn addition on microstructure and tensile properties of Sn-1Ag-0.5Cu alloy", *Materials Science and Engineering A*, 527, (2010), 1343-1350.
19. K. Pietrzak, M. Grobelny, K. Makowska, N. Sobczak, D. Rudnik, A. Wojciechowski, and E. Sienicki, "Structural Aspects of the Behavior of Lead-Free Solder in the Corrosive Solution", *Journal of Materials Engineering and Performance*, 21, 5, (2012), 648-654.
20. M.T. Nawar, B.A. khalifa, G.S. Al-Ganainy, and A.W. Shalaby, "Crystallinity, crystallite size and some physical properties of two fiber maturity levels in some Egyptian cotton cultivars", *Egypt. J. Sol.*, 18, (1), (1995) 61-73.
21. N. Barakat, B.A. Khalifa, F. Sharaf and A. El-Bahy, "X-ray diffraction studies of γ -irradiated Nylon 6 (Polycapramide) fibers", *Egypt. J. Phys.* 15, (2), (1984) 237-246.
22. Carina Morando, Osvaldo Fornaro, Olga Garbellini & Hugo Palacio, "Thermal properties of Sn-based solder alloys", *J Mater Sci: Mater Electron*, 25, 8, (2014), 3440 -3447.
23. A.M. Yassin, R.L. Reuben, G. Saad, M.H.N. Beshai and S.K. Habib, "Effect of annealing and microstructure on the creep behavior of an Sn-10wt%Sb alloy", *Proc. Instn. Mech. Engrs.*, 213, (1999), 59-68.
24. B.A. Khalifa, R. Afify Ismail, A.M. Yassin, "Structure Analysis, Enhancement of Creep Resistance and Thermal Properties of Eutectic Sn-Ag Lead-Free Solder Alloy by Ti and Cd

- Additions", *Journal of Advances Physics*, 1, 8, (2017), 5092-5099.
25. A.A. El-Daly, H. El-Hosainy, T.A. Elmosalami, W.M. Desoky, "Micro-structural modifications and properties of low-Ag-content SnAgCu solder joints induced by Zn alloying", *Journal of Alloys and Compounds*, 653, (2015), 402-410.
 26. Yujin Park, Jung-Hwan Bang, Chul Min Oh, Won Sik Hong and Namhyun Kang, "The Effect of Eutectic Structure on the Creep Properties of Sn-3.0Ag-0.5Cu and Sn-8.0Sb-3.0Ag Solders", *Metals*, 7, (2017), 540.
 27. J. Friedel, "Dislocations", (Pergamon Press, London, 1964); M.T. Mostafa, *Phys. Status Solidi*, A 163, (1997), 39-44.
 28. J.H. Lau, Ed., *Thermal Stress and Strain in Microelectronics Packaging*, van Nostrand Reinhold, New York, chapter 7, "Die Stress Measurement Using Piezoresistive Stress Sensors", by J. N. Sweet, (1993), pp. 221.
 29. J.E. Bird, A. K. Mukherjee and J.E. Dorn, "Quantitative relation between properties and microstructure", (Israel University Press, 1969, 255-261.
 30. A.A. El-Daly, Y. Swilem, AE. Hammad, "Creep properties of Sn-Sb based lead free solder alloys", *J. Alloys Compd.*, 471, 471, (2009), 98-104.